minerals

MDPI

Article

The Memorial Chapel (Formerly Holy Trinity Church) in the *Tempio Evangelico Valdese* (Florence): Surveys and Characterization of Decorative Plasters for a Conservative Recovery

Sara Calandra [1,*], Elena Pecchioni [1,*], Francesca Briani [2], Maria Di Benedetto [3], Carlo Alberto Garzonio [1], Eleonora Pica [1], Teresa Salvatici [1], Irene Centauro [1] and Alba Patrizia Santo [1]

[1] Department of Earth Sciences, University of Florence, 50121 Florence, Italy; carloalberto.garzonio@unifi.it (C.A.G.); eleonora.pica@edu.unifi.it (E.P.); teresa.salvatici@unifi.it (T.S.); irene.centauro@unifi.it (I.C.); alba.santo@unifi.it (A.P.S.)
[2] Adarte S.n.c., Via E. Agnoletti 3, 50141 Florence, Italy; francescabriani@adartesnc.it
[3] Department of Architecture DIDA, University of Florence, 50121 Florence, Italy; maria.dibenedetto@unifi.it
* Correspondence: sara.calandra@unifi.it (S.C.); elena.pecchioni@unifi.it (E.P.)

Abstract: This study focuses on the Memorial Chapel, a historical site located inside the *Tempio Evangelico Valdese* in Florence. In 1843, the first Anglican church in Florence, known as Holy Trinity Church, was built by D. Giraldi. Around 1892, G. F. Bodley began the reconstruction of a new building of neo-Gothic style at the same site, which was completed in 1904. This new church had a space dedicated to memory called Memorial Chapel. In 1967, the monumental complex was acquired by the Waldensians, now known as the *Tempio Evangelico Valdese*. This interdisciplinary investigation aimed to study the most damaged painted walls of the chapel. For this purpose, samples of decorative plaster mortars were collected from various points, after carrying out a digital mapping of the degraded areas. Mineralogical, petrographic, optical, chemical, and microchemical analyses were performed. This study made it possible to highlight the composition and the characteristics of the different layers of the plaster mortars, permitting us also to identify the types of pigments used over time in the paintings; furthermore, it was possible to reconstruct the degradation phenomena on the walls and the events that caused them, providing valuable insight for targeted restoration efforts.

Keywords: Memorial Chapel; plaster mortars; paintings; interdisciplinary analyses

Citation: Calandra, S.; Pecchioni, E.; Briani, F.; Di Benedetto, M.; Garzonio, C.A.; Pica, E.; Salvatici, T.; Centauro, I.; Santo, A.P. The Memorial Chapel (Formerly Holy Trinity Church) in the *Tempio Evangelico Valdese* (Florence): Surveys and Characterization of Decorative Plasters for a Conservative Recovery. *Minerals* **2024**, *14*, 658. https://doi.org/10.3390/min14070658

Academic Editor: Adrián Durán Benito

Received: 21 May 2024
Revised: 20 June 2024
Accepted: 21 June 2024
Published: 26 June 2024

1. Introduction

The analysis of artificial materials, such as mortars, plasters, and/or painted plasters, used in cultural heritage is an essential part of archaeometry and conservation research, as it enables the knowledge of material culture [1–3]. Their characterization can provide information about each component used in the realization and the technologies applied by the craftsmen.

In particular, the study of mortars permits us to identify the raw materials used in their production. For example, the presence of lumps, such as under-burnt stone in the binder, can indicate the limestone used, while the type of the aggregate suggest the supply area.

Regarding the pigments used in the colored finishing layer of the plasters, the study can provide important information on whether they are ancient and/or modern pigments and whether there are multiple layers applied over time. This knowledge is fundamental to the application of pigments suitable for the original materials.

Several studies use minero-petrographic, microchemical, and chemical characterizations to gain important insights into the differentiation of construction phases and restoration processes, and to provide important suggestions for the preservation of cultural heritage [4,5].

The study focuses on the Memorial Chapel, a site of historical–artistic interest and commemorative nature, located inside the *Tempio Evangelico Valdese* on Via P.A. Micheli in Florence [6]. The Memorial Chapel is considered one of the most interesting memorials in Florence, as is the Laurel Cemetery, also known as the English Cemetery. Alongside the Stibbert Museum, they symbolize the presence and influence of a notable foreign community in Florence [7,8].

With the progressive increase of the English people in Florence during the 19th century, the desire arose for a dedicated place of worship. Consequently, in 1843, the first Anglican Church, named Holy Trinity Church, was built in Florence under the architect Domenico Giraldi. Successively, around 1892, the architect George Frederik Bodley initiated the reconstruction of a new building in the neo-Gothic Victorian style, completed in 1904 [7].

The layout of the renovated church, still visible today, consists of a room with three naves, a presbytery in the north wall, a sacristy, and a library situated adjacent to the Church. Additionally, there is a dedicated space for the remembrance, known as Memorial Chapel. In 1967, the monumental complex was handed over by the Anglican community to the Waldensian community and currently bears the name *Tempio Evangelico Valdese*. The Memorial Chapel was retained within the church, representing a space dedicated to the memory, distinct from the present church.

Unlike the decorations on the rest of the church walls, which, following the Waldensian liturgical tradition, were partially covered because they were deemed superfluous, the wall decorations inside the Memorial Chapel are preserved [7–9].

This study focused on investigating a specific area of the chapel's walls, namely the south-southeast wall, which shows an advanced state of degradation, characterized by the loss of decorative integrity and aesthetic appeal of the plaster mortars, along with evident lifting, swelling, and detachment. The aim of this study was to investigate the degraded wall-painted plasters of the Memorial Chapel using an interdisciplinary approach. This is essential given the unique historical significance and interest in preserving this site, ensuring accurate information on its condition of decay. For this purpose, several samples were collected from different areas of the wall and subjected to mineralogical, petrographic, optical, chemical, and microchemical analysis [10,11]. Furthermore, the wall was digitally mapped to highlight missing architectural relief. The study allowed us to identify the phenomenology of degradation taking place on the wall, permitting the reconstruction of the events leading to its appearance and providing a valuable tool for planning targeted restoration interventions [12–14].

Historical Notes on Memorial Chapel

In the 18th century, the presence of a large English community in Florence, "attracted by the presence of artistic and cultural resources" [7,8], encouraged academic trips, known as Grand Tour. However, the English residents were looking for a place to pray. They were hindered by Italy's strict adherence to Catholicism, which tolerated no other religious practices. Only in the 19th century the Grand Duke of Tuscany permitted foreign residents to practice their religious worship in private chapels within Tuscan territory. This was under close supervision, as the conversion of the local population was strictly prohibited [7,8]. Initially, the English community practiced religious worship clandestinely (1815–1820), in private residences. Later, it discovered a small chapel on Via Maggio, sharing it with the Swiss community (1828). It was not until around 1844 that they were able to manage to construct their dedicated church building, the first Holy Trinity Church. This structure was succeeded by the second Bodley-designed building, which now serves as the *Tempio Evangelico Valdese* (Figure 1).

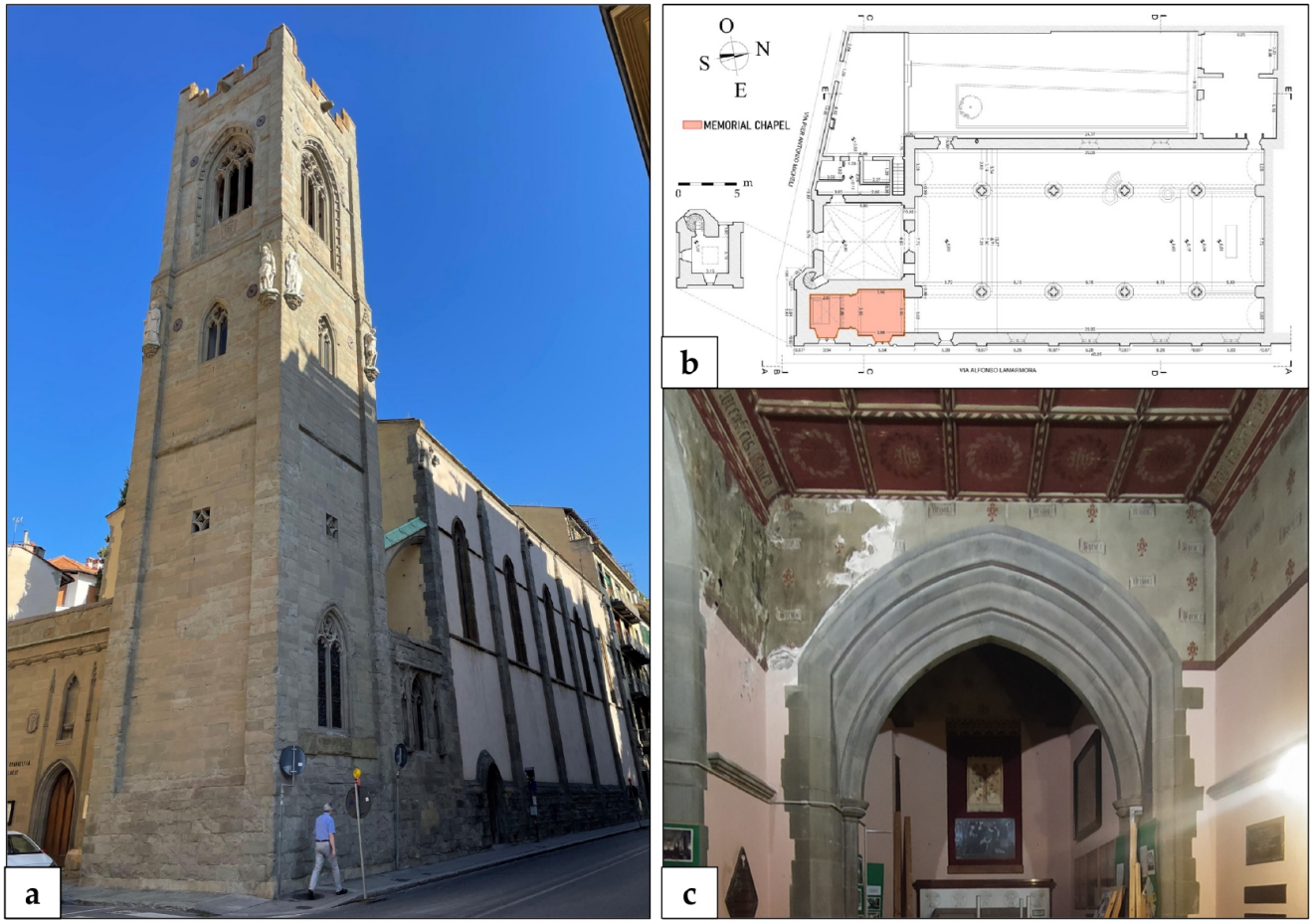

Figure 1. *Tempio Evangelico Valdese* in Florence, where the Memorial Chapel is located (**a**). Plan of the neo-Gothic Anglican church from an architectural survey conducted by architects M. Di Benedetto and F. Nobili (2021); position of the Memorial Chapel is in red (**b**). Investigated plastered walls of the chapel (**c**).

The Memorial Chapel is in the southern and southeastern section of the *Tempio Evangelico Valdese* (Figure 1a,b). The chapel has two mullioned windows, overlooking Via A. La Marmora, realized with stained glass depicting scenes such as Magdalene with Christ and the Annunciation. These windows were crafted by the London firm Burlison and Grylls, established in 1868 by architects G.F. Bodley and T. Garner [9,15].

In the wall paintings of the chapel, Bodley expressed his admiration for the picturesque Middle Ages, referring to the Decorated or ornate Gothic style prevalent in the late 13th century, characterized by rich English colors and decorations (Figure 1c). He enlisted the painters Malesci and Pistolesi who, between 1894 and 1895, decorated the walls of the church with stenciled phytomorphic red designs and scrolls bearing the words "*Kyrie eleison*" (Lord have mercy) on a green backdrop, which today are hidden under a new layer of paint [15].

Inside the Anglican church, the Memorial Chapel was conceived as the place where the English community could honor their loved ones who died in Florence, far from the homeland. Its commemorative character is still evident through the presence of numerous gravestones, an altarpiece, and an altar dedicated to memory. Many gravestone memorials are embedded in the chapel's walls, including one realized in stone, depicting two cherubs in half relief holding a garland that encloses an inscription in memory of David Stanley, Earl of Airlie, who was baptized there in 1856 and died in 1900. Another memorial, made of metal, has a large heraldic emblem in bas-relief, dedicated to the very famous collector Frederik Stibbert [15].

The Memorial Chapel stands as a distinct element within the current *Tempio Evangelico Valdese*, diverging from its decorative style. The chapel remains unused today and is closed to visitors.

2. Materials and Methods

2.1. Sampling of the Degraded Areas

The Memorial Chapel exhibits a high degree of degradation, particularly evident in the left corner of the wall facing south-southeast (Figure 2). Prior to the restoration of the exterior facades (2010–2013), this area suffered significant damage due to both the partial breakage of the adjacent window and fractures in the wall, which facilitated the infiltration of rainwater, leading to moisture exchanges with the external environment. A digital reconstruction of the macroscopic different forms of decay of the plaster mortars on the aforementioned wall was obtained using Agisoft Metashape Professional (Version 1.8.4) and Gimp software (Version 2.10.34) [16–18]. Agisoft Metashape, a photogrammetry software, processes digital images and generates 3D digital environments. Additionally, this software provides detailed documentation and the flat reproduction of walls. Gimp software, an image editor, was employed for a graphical representation of degradation-related information. This software enables the highlighting of degradation areas through synthesized graphics and relevant iconography.

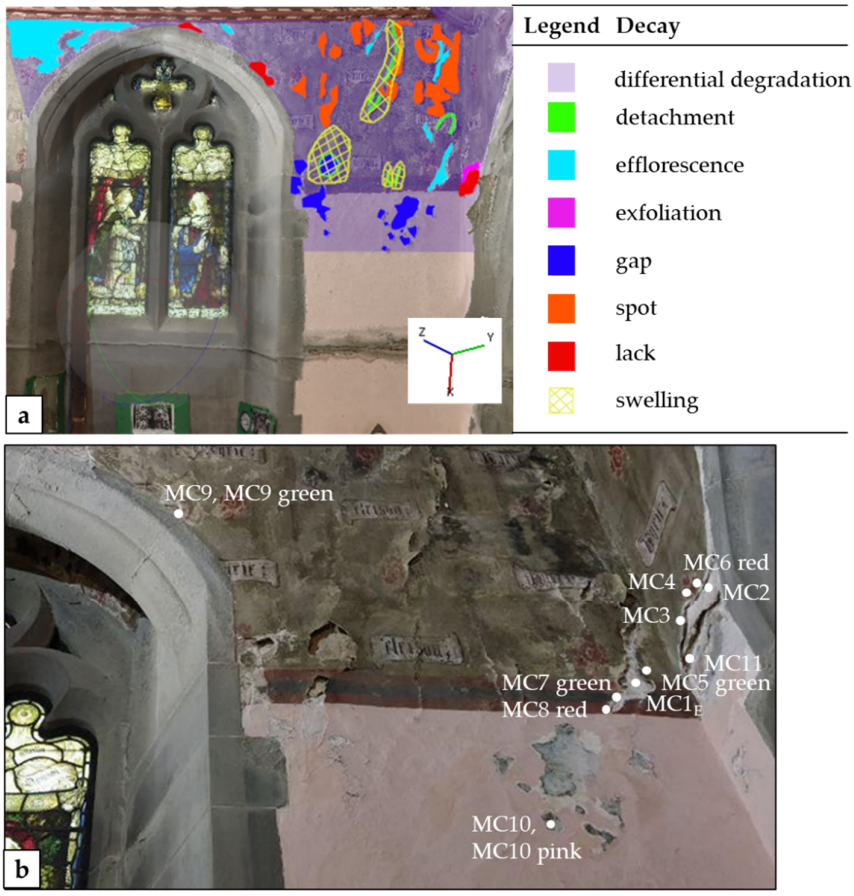

Figure 2. Digital reconstruction of the degraded areas of the chapel's plaster mortars, which allowed a graphic rendering, representing the walls [19] (**a**). Plaster mortars, painted layers, and efflorescence sampled on the south and southeast walls of the chapel (**b**). For the ID sample, see Table 1.

The different forms of degradation were delineated and mapped with distinct colors, shown in Figure 2a, accompanied by a legend and description of the decay phenomena [19]. This graphical documentation facilitated the distinction among the different layers consti-

tuting the plaster mortars: the first layer, *rinzaffo*, which anchors to the masonry; the second layer, named *arriccio*, which serves as levelling mortar; and the finishing layer, named *finitura* [20–23].

The digital reconstruction of the most degraded area allowed us to conduct a more targeted sampling (Figure 2b), enabling a thorough characterization of the various degradation phenomena and types of the samples (Table 1).

The sampling was realized using scalpels and tweezers: plaster mortars (MC2, MC3, MC4, MC9, MC10, MC11), efflorescence salt ($MC1_E$), painted colored layers of the samples MC5 (green), MC6 (red), MC7 (green), MC8 (red), MC9 (green), MC10 (pink), from different areas of the wall were collected. This approach allowed for the verification of the constituent elements used and the evaluation of the state of conservation.

Table 1. List and typology of the samples.

ID Sample	Type	Investigated Material
$MC1_E$	efflorescence	Salt
MC2	*rinzaffo* and *arriccio*	Plaster mortar
MC3	*rinzaffo* and *arriccio*	Plaster mortar
MC4	*rinzaffo* and *arriccio*	Plaster mortar
MC5 green	*finitura*	Painted layer
MC6 red	*finitura*	Painted layer
MC7 green	*finitura*	Painted layer
MC8 red	*finitura*	Painted layer
MC9, MC9 green	*rinzaffo*, *arriccio* and *finitura*	Plaster mortar and painted layer
MC10, MC10 pink	*rinzaffo*, *arriccio* and *finitura*	Plaster mortar and painted layer
MC11	*rinzaffo*	Plaster mortar

Different layers of plaster mortars-*rinzaffo*: anchoring layer to the wall; *arriccio*: levelling layer; *finitura*: finishing layer.

2.2. Thermal Image Analysis

To better understand the degradation phenomena, a thermal imaging camera (Teledyne FLIR E50bx Building Inspection Thermal Camera with 240 × 180 Resolution; Thousand Oaks, CA, USA) was employed to assess the thermal condition of the area (Figure 3a). The measurements were performed during the summer of 2022, with the external temperature ranging between 34 and 38 °C. Figure 3b shows that the average temperature on the wall was 29.3 °C. It was observed that many colder areas (depicted in blue) correspond to regions most affected by detachments and swellings. The crack responsible for the intense degradation in the corner has been properly restored. As a result, both the interior and exterior walls of the chapel now exhibit a similar and constant temperature.

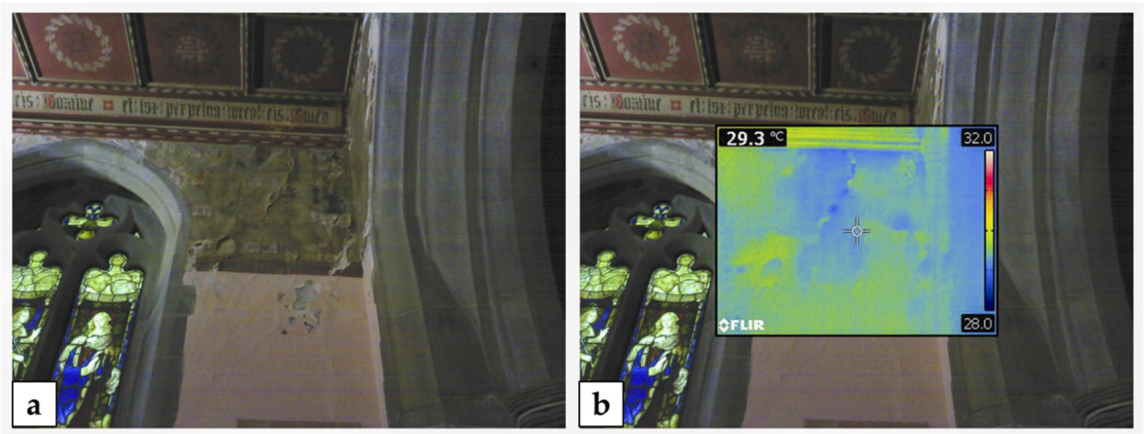

Figure 3. Image of the degraded wall (**a**), and distribution of the temperature revealed by the thermal camera (**b**).

2.3. Analytic Methodologies

The samples were subjected to mineralogical, petrographic, and microchemical analyses.

Petrographic observations in polarized light (PLM) were performed using the microscope Zeiss Axioscope A.1 (Carl Zeiss, Jena, Germany), equipped with a 5-megapixel resolution video camera and Zen lite 3.1 image analysis software. This analysis allowed for the visualization of the binder texture as well as the finer and medium-coarse aggregate characteristics [24]. The same microscope was used to carry out reflected (RLM) and UV light (UVLM) optical observations [25].

Mineralogical qualitative analyses were obtained by X-ray powder diffraction (XRPD) on bulk powder samples of the plaster mortars, using a Philips PW 1050/37 diffractometer (Philips, Almelo, The Netherlands) coupled with a Philips X'Pert PRO system for data acquisition and interpretation. The detection limit for this method is 4%. The operating conditions included 40 kV and 20 mA, a Cu anode, a graphite monochromator, and a goniometer speed of 2 μ/min goniometry in the range of 5–70° 2θ [26–28].

Chemical analysis was performed using Fourier transform infrared spectroscopy (FTIR) in attenuated total reflectance (ATR) mode with a Spectrum 100 FTIR spectrometer (Perkin Elmer Inc., Norwalk, CT, USA). The acquisition was carried out at room temperature in the spectral range between 4000 and 400 cm^{-1}, with 4 repeated scans and a resolution of 4 cm^{-1}. Data acquisition and processing were managed using Spectrum 100 software.

Scanning Electron Microscope Energy-Dispersive Spectroscopy (SEM-EDS) analyses were performed to obtain semi-quantitative microchemical composition and textural characterizations [29]. A scanning electron microscope (SEM) ZEISS EVO MA 15 (Carl Zeiss, Jena, Germany) equipped with a W filament and an analytical system in the dispersion of energy (EDS/SDD), specifically the Oxford Ultimax 40 (with a 40 mm^2 area and resolution of 127 eV 5.9 keV), was employed. The measurements were conducted on thin sections after carbon-metallized treatment. The operating conditions were as follows: 15 kV acceleration potential, 500 pA beam current, 9–8.5 mm working distance. For point analyses, a 20 s live-time acquisition rate was employed to achieve at least 600,000 cts on a Co standard, a processing time of 4 was used for map acquisition, and a 500 μs pixel dwell time with a resolution of 1024 × 768 pixels was used.

The microanalysis was carried out using Aztec 5.0 SP1 software, utilizing the XPP matrix correction scheme developed by Pouchou and Pichoir [30]. The process used acquired standard elements for calculations, enabling "standard-less" quantitative analysis. The use of numerous analyses of a cobalt metallic standard permitted the documentation of constant analytical conditions (i.e., filament emission).

3. Results

3.1. Petrographic Results (PLM)

The results of the petrographic analysis of the plaster mortars have highlighted the textural characteristics of the three different layers (*rinzaffo*, *arriccio*, and *finitura*) (Figure 4a) constituting the samples [31–34].

The samples of *finitura* (MC5, MC6, MC7, MC8, MC9, MC10) show a typical fine superficial layer constituted by lime whitewashing added with distinct colors (Figure 4b, sample MC9). The samples MC2, MC3, MC4, MC9, and MC10, with both *arriccio* and *rinzaffo* layers, show no differences between them or between the two layers, except for the variation in the grain size of the aggregate, which is larger in the *rinzaffo* layer. Both layers consist of a binder made of an air-hardening calcic lime, with Havana color, displaying an anisotropic appearance and a micritic texture, with small dark inclusions. These latter are characteristics of natural hydraulic lime, often dispersed in a micritic binder, in low amounts. They are referable to non-completely crystallized compounds of non-hydrated calcium/aluminum silicate, due to the presence of the clay components in low quantity in the limestone. The aggregate has heterogeneous dimensions in the range of 200–600 μm in the *arriccio* and 700–1000 μm in the *rinzaffo* layer (Figure 4b and 4c, respectively, samples MC9 and MC2). The aggregate particles are sub-rounded and sub-angular in shape, well

distributed, and predominantly composed of fragments of quartz crystals, micas, iron oxides, carbonate rock (including remnants of Alberese Limestone of approximately 1 mm) (Figure 4c), sandstone, quartzite, and rare fragments of *cocciopesto*. Some lumps of unmixed lime and under-burnt limestone are also visible, highlighting a traditional manufacturing technique. The macro-porosity of the samples observed in the thin sections is medium to high, with a binder/aggregate ratio (L/A) of approximately 1/3.

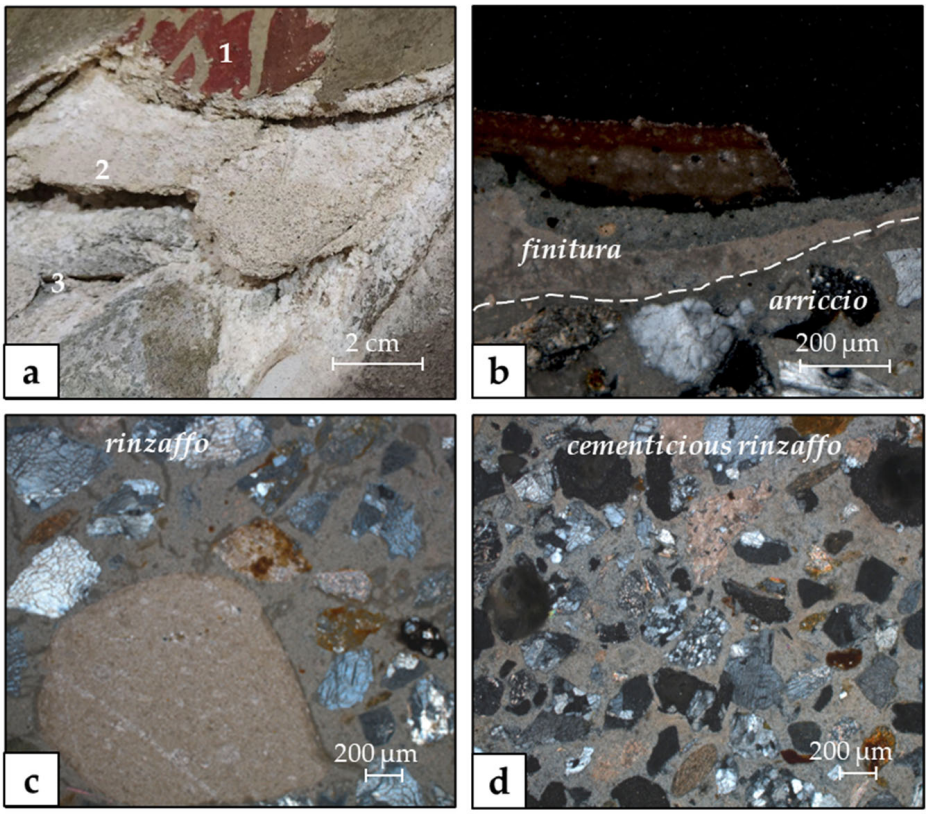

Figure 4. Macro image of the three layers of the plaster mortars on the wall: 1: *finitura*, 2: *arriccio*, 3: *rinzaffo* (**a**). Microscope images in cross-polarized light (PLM) (**b**–**d**): sample MC9 showing the two layers of the plaster mortar: *finitura*—lime whitewashing with different painting colors is visible, and *arriccio*—binder made of air-hardening calcic lime (**b**); sample MC2: *rinzaffo* with a typical Havana color of the binder and a remnant of Alberese Limestone are visible (**c**); sample MC11: cementitious *rinzaffo*, hydraulic binder of grey color with rounded porosity is highlighted (**d**).

The sample MC11 (*rinzaffo*) differs from the others. It shows a hydraulic binder of grey color, an anisotropic appearance, and a micro-sparitic texture. Within the binder, abundant small dark inclusions, constituted by non-hydrated relicts of calcium/aluminum silicate (i.e., belite), medium-high relief, shaded contours, and sub-idiomorphic habitus are observed [32,35,36]. The aggregate has a sub-angular and sub-rounded shape with dimensions in the range of 200–600 µm, well distributed. The composition of the aggregate comprises fragments of quartz crystals, feldspars, and micas, along with fragments of sandstones, quartzites, pelites, and limestones. The macro-porosity is sub-rounded and not high, with no cracks present. The binder/aggregate ratio (L/A) is approximately 1/3 (Figure 4d, sample MC11).

3.2. Mineralogical Results (XRPD)

The results of the mineralogical analyses (qualitative analysis with partial estimate of the minerals' amounts based only on peak elongation) are listed in Tables 2 and 3. The data have been divided into two types, one relating to plaster mortars and efflorescence, and the other to the colored painted layers. All collected spectra are reported in Figure S1.

Table 2. Qualitative mineralogical composition (XRPD) of the plaster mortars and efflorescence.

Sample	Cal	Qz	Pl	Kfs	Gp	Phyllosilicates	Mrb
$MC1_E$	x	xx	-	-	x	tr	xx
MC2	xx	xxx	xx	x	-	tr	-
MC3	xx	xx	x	-	x	tr	-
MC4	xx	xx	xx	-	tr	-	-
MC9	xx	xxx	x	x	-	tr	-
MC10	xx	xx	x	-	tr	-	-
MC11	xx	xxx	xx	x	x	tr	-

Cal = calcite; Qz = quartz; Pl = plagioclase; Kfs = K-feldspar; Gp = gypsum; Mrb = mirabilite; E = efflorescence; xxx = high amount; xx = medium amount; x = low amount; tr = traces; - = absent.

Table 3. Qualitative mineralogical compositions (XRPD) of the colored layers.

Sample	Znc	Gp	Anh	Qz	Cal	Brt	Sdl	Others
MC5 green	x	xx	x	x	xx	tr	tr	-
MC6 red	-	x	-	xx	xx	-	-	Pl (tr)
MC7 green	-	xx	tr	x	tr	tr	tr	Pl (tr)
MC8 red	-	xx	-	tr	x	tr	x	-
MC9 green	-	xx	-	xx	xx	x	tr	Phc (tr)
MC10 pink	-	x	tr	tr	xxx	tr	tr	Ang (tr)

Znc = zincite; Gp = gypsum; Anh = anhydrite; Qz = quartz; Cal = calcite; Brt = barite; Sdl = sodalite; Pl = plagioclase; Phc = phoenicochroite; Ang = anglesite; xxx = high amount; xx = medium amount; x = low amount; tr = traces; - = absent.

The mineralogical analyses highlighted the prevalent presence of mirabilite ($Na_2SO_4 \cdot 10H_2O$) and gypsum ($CaSO_4$ $2H_2O$) in sample $MC1_E$ (efflorescence) in addition to the components of the underlying plaster mortar (calcite, quartz, and phyllosilicates). Samples MC2, MC3, MC4, MC9, MC10, and MC11 have similar mineralogical compositions, characterized by a prevalence of quartz, calcite, plagioclase, and K-feldspar. Additionally, MC2, MC3, MC9, and MC11 contain traces of micas and clay minerals, while gypsum is present in low or trace amounts in MC3, MC4, MC10, and MC11. As regards the analyses of the colored painted surfaces, it is important to underline that in all samples are present calcite, quartz, and gypsum. Sample MC5 green shows the presence of zincite (ZnO), anhydrite ($CaSO_4$), barite ($BaSO_4$), and sodalite ($Na_8(Al_6Si_6O_{24})Cl_2$). In MC6 red, traces of plagioclase are also detected. Sample MC7 green contains barite, sodalite, and plagioclase, while MC8 red shows the presence of barite and sodalite, and MC9 green shows barite, sodalite, and phoenicochroite ($Pb_2(CrO_4)O$). Lastly, MC10 pink contains barite, sodalite, and anglesite ($PbSO_4$).

3.3. Chemical Results (ATR-FTIR)

The results of the chemical analysis obtained by infrared spectroscopy in attenuated total reflectance mode (ATR-FTIR) on the painted layers' samples were plotted and are shown in Figure 5a.

The spectral band assignments show that the samples consist of gypsum, calcite, and silicates (highlighted in Figure 5a, in grey, red, and yellow, respectively), consistent with the XRPD analysis. Additionally, characteristic peaks of organic compounds can also be observed (Figure 5b). Comparing the spectra, MC5 green and MC7 green exhibit similarities, displaying weak bands around 3000–2800 cm^{-1} (assigned to ν (CH_2, CH_3, CH)) and at 1736 cm^{-1} (assigned to ν (C=O)), which are attributed to organic compounds (highlighted with asterisks in Figure 5b). These bands are not visible in sample MC9 green, which shows a peak at 2083 cm^{-1}, possibly related to the stretching vibration of the C≡N bond (highlighted with an asterisk in Figure 5b), which is typical of cyanide groups in organic and inorganic compounds and may be indicative of ultramarine blue [37]. Comparing the spectra of MC6 red and MC8 red, they are similar and show weak bands around 3000–2800 cm^{-1}. The spectrum of sample MC10 pink is indicative of predominant

calcite, with gypsum. The peak at 1736 cm^{-1} and the shoulder at 1240 cm^{-1} (highlighted with asterisks in Figure 5b) are possibly related to the stretching vibration of the C-N bond. However, further analysis is required to confirm this interpretation.

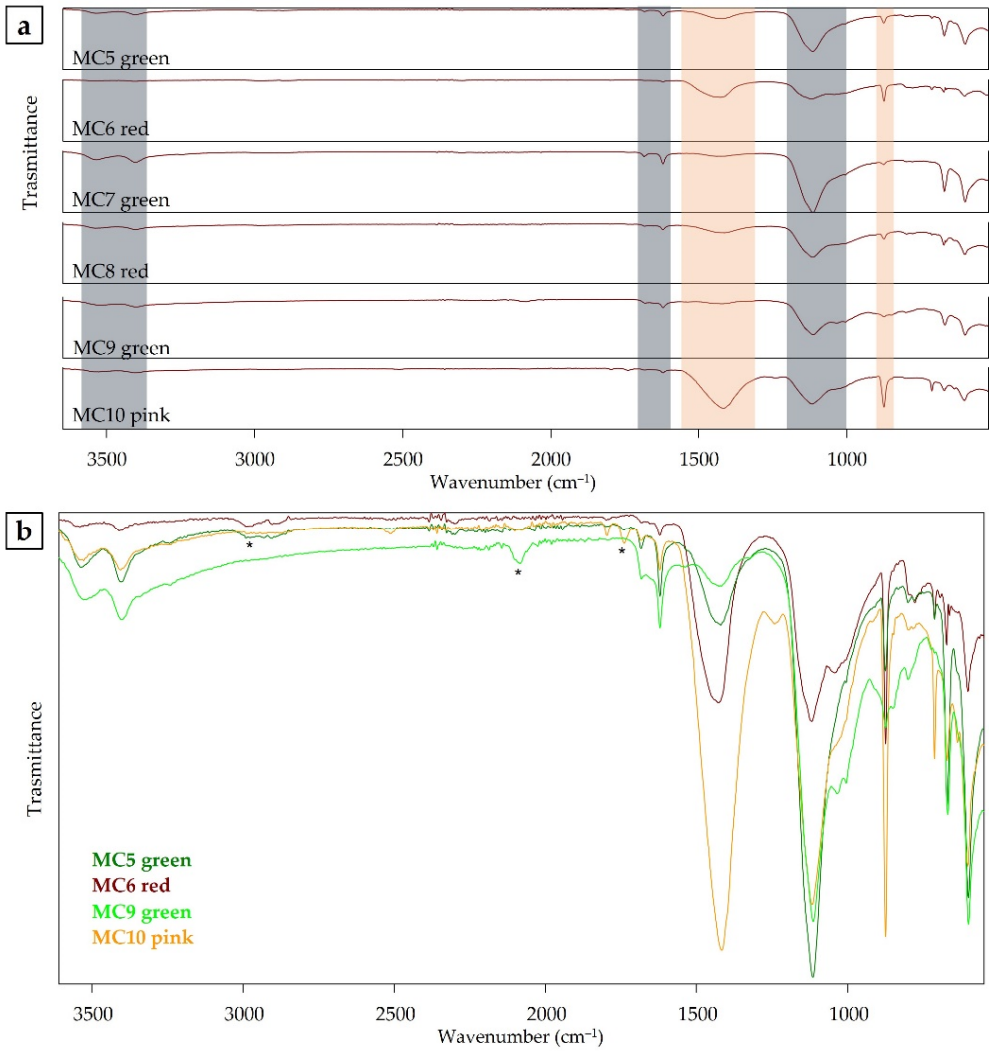

Figure 5. Detail of the ATR-FTIR spectra of colored surface samples (range of interest 3600–500 cm^{-1}) with attribution: grey—gypsum; red—calcite (**a**); ATR spectrum with highlighted bands. The FTIR spectra of four representative samples show the presence of organic compounds, which are highlighted with an asterisk (**b**).

3.4. Optical and Microchemical Results (RLM, UVLM, SEM-EDS)

The results of the observations under reflected and UV light using the optical microscope are reported together with the data obtained through SEM-EDS analyses. This combined approach allowed us to highlight more matching between SEM-EDS greyscale images, where it is difficult to distinguish the single-colored layers, and color images from reflected and UV light microscopy. The results of these analyses are summarized in Figure 6, where the samples representative of different surface colors found in the painted wall (green, red, and pink) are shown [38]. The collected EDS spectra are reported in Figures S2–S4.

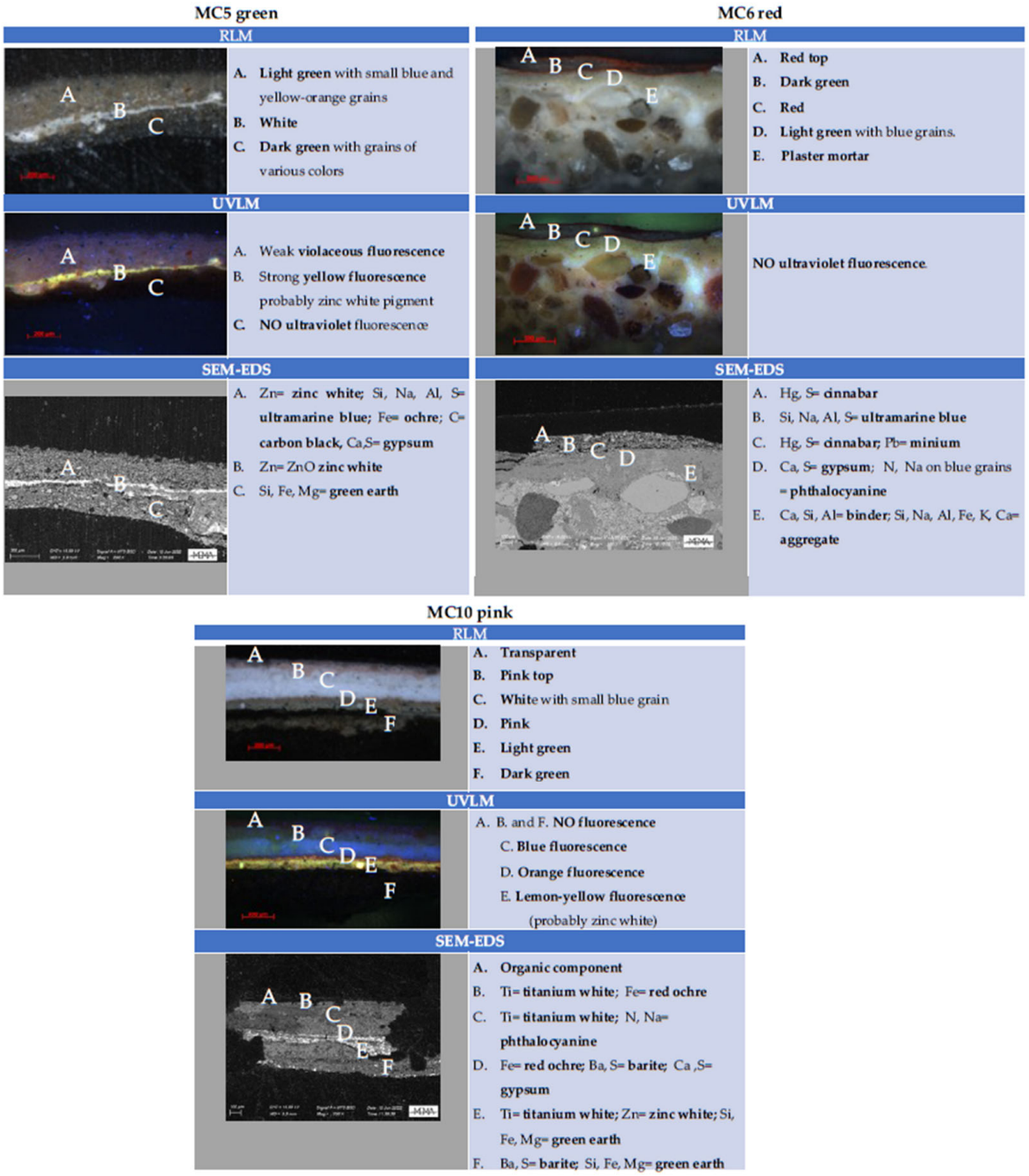

Figure 6. The image shows the microscopical data obtained on three painted samples (MC5 green, MC6 red, MC10 pink) with different surface colors. For each sample, the different stratigraphy of the color layers was highlighted through the optical microscope observation: RLM, UVLM, and analysis: SEM-EDS.

Sample MC5 green presents, in reflected light, three different layers, arranged from the surface downwards: a light green layer containing blue and yellow-orange grains, followed by a white layer, and underneath, a dark green layer with grains of various colors. Microscopic observations under UV light again confirmed the different stratigraphy: the top layer with weak violaceous fluorescence, the middle layer with strong yellow fluorescence, and the bottom layer showed no ultraviolet fluorescence. SEM-EDS analysis allowed us to identify the chemical composition of each layer. The first green layer contains Zn, likely due to zinc white (zinc oxide), Si, Na, Al, and S, attributed to ultramarine blue pigment ($Na_{8–10}Al_6Si_6O_{24}S_{2–4}$), responsible also for the blue grains, Fe from ochre (Fe_2O_3), C from

carbon black, and Ca and S, indicative of gypsum. In the middle layer, Zn is again present, possibly due to the use of zinc white. At the bottom, Si, Fe, and Mg are probably due to the use of a green earth (Figure S2). Green earth contains phyllosilicate and is suitable for painting in any medium for stable and non-reactive properties. The green color is caused by the presence of Fe-containing minerals (i.e., celadonite, glauconite, and smectites) [39].

Sample MC6 red shows, in reflected light, four layers that appear from top to bottom: red, dark green, red, and light green with blue grains. Microscopic observations in UV do not show any fluorescence. SEM-EDS analysis highlights the chemical composition of each layer: Hg and S, probably from cinnabar (HgS) are found in the top layer; Si, Na, Al, and S, attributed to ultramarine blue pigment, are found in the second layer; the third layer contains Hg (likely from cinnabar) and Pb, indicative of minium (Pb_3O_4); in the bottom layer, Ca and S from gypsum and N and Na on blue grains, possibly attributed to phthalocyanine ($C_{40}H_{23}N_7O_{13}S_4 \cdot 4Na$), are present (Figure S3).

Sample MC10 pink shows six overlapping layers in reflected light: transparent, pink, white (with small blue grains), pink, light green, and dark green. The first, second, and last layers do not exhibit fluorescence under UV light, while the third layer shows blue fluorescence, the fourth layer shows orange fluorescence, and the fifth layer displays lemon-yellow fluorescence. SEM-EDS analysis shows in the top layer an organic component. The second layer contains Ti, indicative of titanium white (TiO_2), and Fe, of red ochre (Fe_2O_3). The third layer still shows Ti for titanium white and N and Na, possibly due to the presence of phthalocyanine. The fourth layer contains Fe for red ochre, Ba and S, likely for barite, and Ca and S, for gypsum. In the bottom layer are present Ti from titanium white, Zn from zinc white, and Si, Fe, and Mg, attributed to the presence of green earth pigment (Figure S4).

4. Discussion

The minero-petrographic data have revealed a traditional manufacturing process for plaster mortars constituting the *finitura*, *arriccio*, and *rinzaffo* of the wall. The layers of *finitura* are constituted of a *scialbo* of calcium carbonate on which different colored pigments were applied. The *arriccio* and *rinzaffo* plasters show no differences between them, except for the different grain sizes of the aggregate, larger in the *rinzaffo*. The carbonate lime binder in both layers was probably obtained by burning Alberese Limestone, as fragments of this under-burnt limestone are often present. Alberese Limestone was widely utilized in buildings due to its marly limestone nature, which cropped out in Tuscany, and it allowed the production of lime with weak hydraulic characteristics [40]. However, sample MC11 (part of the internal wall) is different from the others: the binder characteristics are typical of a cementitious hydraulic binder, having a micro-sparitic texture, rounded porosity, grey color, and the presence of small dark inclusions constituted by non-hydrated relicts of calcium/aluminum silicate (i.e., belite). All samples contain a similar aggregate, consisting of feldspathic quartz sand. The rare presence of gypsum is considered of secondary origin, likely due to degradation phenomena (sulfatation).

In the efflorescence sample ($MC1_E$), the mineralogical data revealed the presence of salts such as mirabilite and gypsum. These minerals can be mainly attributed to sulfation resulting from the use of cementitious binders (see sample MC11) [35] and from atmospheric pollution phenomena [41]).

The chapel, although a closed environment, experienced, before the exterior restoration of the church, conditions such as broken windows, fractures in the walls, and water percolations, allowing exchanges with the outside environment. The wall where the efflorescence is observed likely had a relative humidity (RH) greater than 70%, and a temperature lower than 32.4 °C, conditions that allow the formation of mirabilite, according to many authors [42–44]. The sample $MC1_E$ was collected in January when the temperature was lower than 32.4 °C and the humidity was probably high, as indicated by the moist state of the sample, which explains the presence of mirabilite. The poor state of conservation of the wall suggests thermohygrometric variations in the past that could have permitted the

transformation of mirabilite into thenardite (Na_2SO_4) and vice versa, causing significant cracking. Indeed, the transitions from the anhydrous (thenardite) to hydrated (mirabilite) phase of sodium sulfate can generate a considerable pressure of crystallization and expansion given by the 315% increase in volume [42,45]. The measurements carried out in the summer of 2022 after the external restorations of the *Tempio Evangelico Valdese* suggest that current temperature conditions inside the chapel are constant (always lower than 32.4 °C) and that the presence of mirabilite is "stable".

The microscopic analyses conducted in polarized, reflected, and UV light revealed different stratigraphic layers of color, placed over time. SEM-EDS data allowed us to define the composition and types of color pigments [46]. These pigments are mainly of modern origin and industrial production, likely between the 19th and 20th centuries [47]. Indeed, the presence of titanium white, zinc white, phthalocyanine, and barite confirm the industrial origin of the pigments. However, barite could be related also to a consolidant treatment with the barium hydroxide method. This treatment, carried out on wall paintings, facilitates the formation of barium sulfate (barite) along with other products, as seen in [48]. Barium sulfate formation is also favored by the presence of gypsum, found in these painted layers. The barite promotes the consolidation process, being an insoluble salt, and also produces calcium carbonate.

The ultramarine blue, carbon black, minium, and cinnabar pigments could be natural but the overlap with modern ones suggests otherwise. The green earth, found in the sample MC5 green, could be the only natural pigment, given its location at the base of the colored layers.

XRPD analyses of the colored surface have detected and confirmed the presence of zincite (see sample MC5 green) for zinc white and barite and sodalite, with the latter possibly attributed to the small blue-colored grains within the pigments (see sample MC10 pink), while in the case of the barite, it could be attributed to the production of the paintings or to the use of consolidant treatment. Lead minerals such as phoenicochroite and anglesite are present in the samples MC9 green and MC10 pink, possibly as constituents of the white pigments [49]. The gypsum detected on the colored layers is of secondary origin, due to degradation processes such as sulfation. The damage in the exterior facade facilitated exchanges with the outdoor polluted environment, giving rise to gypsum.

ATR-FTIR data indicated the presence of organic phases, likely ageing of a medium [50] within all the colors. Further investigations should be carried out to highlight the kind of organic compound used in this context.

5. Conclusions

The analyses conducted on the plaster mortars wall (south-southeast) have enabled the characterization of constituent materials and identification of the present decay phenomena. The degradation map was superimposed onto the 3D model obtained through photogrammetry using Agisoft Metashape Professional software (Version 1.8.4). The degradation areas were then delineated using the graphics software Gimp (Version 2.10.34). The minero-petrographic data indicated a traditional manufacturing technique for plaster mortars of *finitura*, *arriccio*, and *rinzaffo* layers. The *finitura* layers consist of a *scialbo* of calcium carbonate and colored pigments, while the *arriccio* and *rinzaffo* layers were produced by burning Alberese Limestone, resulting in a weak hydraulic air lime. The aggregate used is a feldspathic quartz sand. Sample MC11 (collected from the internal wall) represents a cementitious mortar, evidenced by the presence of white efflorescence (mirabilite and gypsum), indicative of both a cementitious mortar composition (likely used in a previous repair), and the humidity of the masonry. Environmental conditions inside the church, following recent restoration works conducted externally, have stabilized. Observations in reflected light have revealed different stratigraphic painted layers, suggesting the application of multiple color coats over time. The XRPD, ATR-FTIR, and SEM-EDS data confirm the OM observations, indicating predominantly modern industrial pigments (from the 19th to the 20th century), although some natural pigments, particularly the green (green earth),

may also be present at the base of the colored stratigraphy. These pigments are bound together by an organic medium. The obtained data provide a valuable tool for a targeted recovery of this chapel dedicated to memory.

Supplementary Materials: The following supporting information can be downloaded at https://www.mdpi.com/article/10.3390/min14070658/s1, Figure S1. Series of XRPD spectra of salt (MC1E), plaster mortar (MC2, MC3, MC4, MC9, MC10, MC11), and painted layer samples (MC5 green, MC6 red, MC7 green, MC8 red, MC9 green, MC10 pink). Figure S2. The collected EDS spectra of the MC5 green painted layers are reported (a–c). BSE image of layered area (d). Figure S3. The collected EDS spectra of the MC6 red painted layers are reported (a–e). BSE image of layered area (f). Figure S4. The collected EDS spectra of the MC10 pink painted layers are reported (a–e). BSE image of layered area (f).

Author Contributions: Conceptualization, E.P. (Elena Pecchioni), F.B., S.C., T.S., E.P. (Eleonora Pica), M.D.B. and A.P.S.; methodology, E.P. (Elena Pecchioni), F.B., S.C., T.S., E.P. (Eleonora Pica), M.D.B. and A.P.S.; software, E.P. (Elena Pecchioni), F.B., S.C., T.S., E.P. (Eleonora Pica), M.D.B., A.P.S. and I.C.; validation, E.P. (Elena Pecchioni), F.B., S.C., T.S., E.P. (Eleonora Pica), M.D.B., A.P.S., I.C. and C.A.G.; formal analysis, E.P. (Elena Pecchioni), F.B., S.C., E.P. (Eleonora Pica) and M.D.B.; investigation, E.P. (Elena Pecchioni), F.B., S.C., E.P. (Eleonora Pica) and M.D.B.; data curation, E.P. (Elena Pecchioni), F.B., S.C., T.S., E.P. (Eleonora Pica), M.D.B., A.P.S., I.C. and C.A.G.; writing—original draft preparation, E.P. (Elena Pecchioni), F.B., S.C., E.P. (Eleonora Pica) and A.P.S.; writing—review and editing, E.P. (Elena Pecchioni), F.B., S.C., T.S., E.P. (Eleonora Pica), M.D.B., A.P.S., I.C. and C.A.G.; visualization, E.P. (Elena Pecchioni), F.B., S.C., T.S., E.P. (Eleonora Pica), M.D.B., A.P.S., I.C. and C.A.G.; supervision, E.P. (Elena Pecchioni), F.B., S.C., T.S., E.P. (Eleonora Pica), M.D.B., A.P.S., I.C. and C.A.G. All authors have read and agreed to the published version of the manuscript.

Funding: This research received no external funding.

Data Availability Statement: Data are contained within the article and Supplementary Materials.

Acknowledgments: Our thanks go to Andrea Todorow, Cultural Heritage Conservator, for his availability in providing us with all the historical information and for his help with the sampling, and to Marco Santini and *Chiesa Evangelica Valdese* and its Consistory in Florence, for allowing us to carry out the studies inside the Memorial Chapel.

Conflicts of Interest: Francesca Briani is an employee of Adarte S.n.c. The paper reflects the views of the scientists and not the company.

References

1. Pecchioni, E.; Pallecchi, P.; Giachi, G.; Calandra, S.; Santo, A.P. The Preparatory Layers in the Etruscan Paintings of the Tomba dei Demoni Alati in the Sovana Necropolis (Southern Tuscany, Italy). *Appl. Sci.* **2022**, *12*, 3542. [CrossRef]
2. Armetta, F.; Giuffrida, D.; Ponterio, R.C.; Martinez, M.F.F.; Briani, F.; Pecchioni, E.; Santo, A.P.; Ciaramitaro, V.C.; Saladino, M.L. Looking for the Original Materials and Evidence of Restoration at the Vault of the San Panfilo Church in Tornimparte (AQ). *Appl. Sci.* **2023**, *13*, 7088. [CrossRef]
3. Moskalova, K.; Lyashenko, T.; Aniskin, A.; Orešković, M. Modelling the Influence of Composition on the Properties of Lightweight Plaster Mortar and Multicriteria Optimisation. *Materials* **2023**, *16*, 2846. [CrossRef]
4. Briani, F.; Caridi, F.; Ferella, F.; Gueli, A.M.; Marchegiani, F.; Nisi, S.; Paladini, G.; Pecchioni, E.; Politi, G.; Santo, A.P.; et al. Multi-Technique Characterization of Painting Drawings of the Pictorial Cycle at the San Panfilo Church in Tornimparte (AQ). *Appl. Sci.* **2023**, *13*, 6492. [CrossRef]
5. Bracci, S.; Cantisani, E.; Conti, C.; Magrini, D.; Vettori, S.; Tomassini, P.; Marano, M. Enriching the knowledge of Ostia Antica painted fragments: A multi-methodological approach. *Spectrochim. Acta A Mol. Biomol. Spectrosc.* **2022**, *265*, 120260. [CrossRef] [PubMed]
6. Pecchioni, E.; Vettori, S.; Cantisani, E.; Fratini, F.; Ricci, M.; Garzonio, C.A. Chemical and mineralogical studies of the red chromatic alteration of Florentine Pietra Serena sandstone. *Eur. J. Mineral.* **2015**, *28*, 449–458. [CrossRef]
7. Sciclone, G. *Dalla Holy Trinity alla Chiesa Valdese di Firenze*; L'Immagine: Firenze, Italy, 2004.
8. Artini, A. *Archivio Storico*; Polistampa: Firenze, Italy, 2008; 184p.
9. Copinger, W.F. *Holy Trinity Church, Florence, Forty Years of His History (1905–1945)*; L'Impronta: Firenze, Italy, 1946; 115p.
10. Martinet, G.; Quenée, B. Proposal for a useful methodology for the study of ancient mortars. In Proceedings of the RILEM TC-167COM International Workshop, Historic Mortars: Characteristics and Tests, Paisley, UK, 12–14 May 1999; Bartos, P., Groot, C., Hughes, J.J., Eds.; Chapman & Hall: London, UK, 1999; pp. 81–91.

11. Artioli, G. Let the walls speak. A brief history of binders in architecture. In *Rendiconti Accademia Nazionale delle Scienze detta dei XL Memorie di Scienze Fisiche e Naturali*; Libreria Universitaria: Rome, Italy, 2017; Volume XLI, Parte II, Tomo I; pp. 7–18.
12. Matteini, M.; Moles, A. *Scienza e Restauro: Metodi di Indagine*, 7th ed.; Nardini: Firenze, Italy, 1994; 320p.
13. Fitzner, B.; Heinrichs, K. Damage Diagnosis on Stone Monuments-Weathering Forms, Damage Categories and Damage Indices. In Proceedings of the International Conference Stone Weathering and Atmospheric Pollution Network (SWAPNET 2001), Prachov Rocks, Czech Republic, 7–11 May 2001; pp. 11–56.
14. Matteini, M.; Moles, A. *La Chimica nel Restauro. I Materiali dell'Arte Pittorica*, 2nd ed.; Nardini: Firenze, Italy, 2007; 380p.
15. Trotta, G. *Luoghi di Culto non Cattolici nella Toscana dell'Ottocento*; Becocci-Scala: Firenze, Italy, 1997; 79p.
16. Agisoft LLC. Agisoft Metashape User Manual: Professional Edition. Available online: https://www.agisoft.com (accessed on 15 February 2024).
17. The Software Architecture of the GIMP. Available online: https://www.semanticscholar.org/paper/The-Software-Architecture-of-the-GIMP-Oliver-Ruiz/51e9312a8c6376dd0b87e102422acff4c7209d19 (accessed on 15 February 2024).
18. GNU Image Manipulation Program—User Manual. Available online: https://docs.gimp.org/2.10/it/ (accessed on 15 February 2024).
19. *UNI 11182:2006*; Beni Culturali, Materiali Lapidei Naturali ed Artificiali. Descrizione della Forma di Alterazione—Termini e Definizioni. UNI (Ente Nazionale Italiano Unificazione): Milano, Italy, 2006.
20. Cagnana, A. *I Leganti, gli Intonaci, gli Stucchi, in Archeologia dei Materiali da Costruzione. Manuali per l'Archeologia*; S.A.P. s.r.l.: Mantova, Italy, 2000; pp. 284–2000.
21. Arcolao, C. *Le Ricette del Restauro. Malte, Intonaci, Stucchi dal XV al XIX Sec.*, 2nd ed.; Marsilio: Venezia, Italy, 2001; 284p.
22. Pecchioni, E.; Fratini, F.; Cantisani, E. *Le Malte Antiche e Moderne tra Tradizione e Innovazione*, 2nd ed.; Pàtron: Bologna, Italy, 2018; 231p.
23. *UNI-10924;* Conservazione del Patrimonio Culturale—Malte per Elementi Costruttivi e Decorativi—Classificazione e Terminologia. Ente Nazionale Italiano di Normazione: Milano, Italy, 2023.
24. *UNI EN 12407*; Natural Stone Test Methods—Petrographic Examination. Ente Nazionale Italiano di Normazione: Milano, Italy, 2007.
25. Lalli, C. *Analisi Stratigrafiche su Campioni in Sezioni Lucide e Sezioni Sottili/Stratigraphic Analyses of Ancient Works of Art on Samples in Cross Sections and Thin Sections*; OPD Restauro n. 11; Centro Di Della Edifimi srl: Florence, Italy, 1999; pp. 207–216.
26. *UNI EN 13925-1*; Non-Destructive Testing—X-ray Diffraction from Polycrystalline and Amorphous Material—Part 1: General Principles. Ente Nazionale Italiano di Normazione: Milano, Italy, 2006.
27. *UNI EN 13925-2*; Non-Destructive Testing—X-ray Diffraction from Polycrystalline and Amorphous Materials—Part 2: Procedures. Ente Nazionale Italiano di Normazione: Milano, Italy, 2006.
28. *UNI-EN 13925-3*; Non-Destructive Testing—X-ray Diffraction from Polycrystalline and Amorphous Materials—Part 3: Instruments. Ente Nazionale Italiano di Normazione: Milano, Italy, 2006.
29. Lanterna, G. *L'Uso del SEM nella Scienza della Conservazione/The Use of SEM in Science for Conservation*; OPD Restauro n. 11; Centro Di Della Edifimi srl: Florence, Italy, 1999; pp. 39–58.
30. Pouchou, J.L.; Pichoir, F. Quantitative Analysis of Homogeneous or Stratified Microvolumes Applying the Model "PAP". In *Electron Probe Quantitation*; Springer: Boston, MA, USA, 1991; pp. 31–75.
31. Ponce-Anton, G.; Arizzi, A.; Zuluaga, M.C.; Cultrone, G.; Ortega, L.A.; Mauleon, J.A. Mineralogical, textural and physical characterisation to determine deterioration susceptibility of Irulegi Castle lime mortars (Navarre, Spain). *Materials* **2019**, *12*, 584. [CrossRef] [PubMed]
32. Pecchioni, E.; Fratini, F.; Cantisani, E. *Atlas of Ancient Mortars in Thin Section under Optical Microscope*, 2nd ed.; Nardini: Firenze, Italy, 2020; 78p.
33. Arizzi, A.; Cultrone, G. Mortars and plasters—How to characterize hydraulic mortars. *Archaeol. Anthropol. Sci.* **2021**, *13*, 144. [CrossRef]
34. Cantisani, E.; Fratini, F.; Pecchioni, E. Optical and Electronic Microscope for Minero-Petrographic and Microchemical Studies of Lime Binders of Ancient Mortars. *Minerals* **2022**, *12*, 41. [CrossRef]
35. Hewlett, P.C. *Lea's Chemistry of Cement and Concrete*, 4th ed.; Elsevier Butterworth Heineimann: Oxford, UK, 2004; 1057p.
36. Weber, J.; Köberle, T.; Pintér, F. Methods of microscopy to identify and characterise hydraulic binders in historic mortars—A methodological approach. In Proceedings of the 3rd Historical Mortar Conference, Glasgow, UK, 11–14 September 2013; pp. 1–8.
37. Corradini, M.; de Ferri, L.; Pojana, G. Spectroscopic characterization of commercial pigments for pictorial retouching. *J. Raman Spectrosc.* **2021**, *52*, 35–58. [CrossRef]
38. Becucci, M.; Lofrumento, C.; Parfenov, V.; Ricci, M.; Rogozny, M.; Pakhunov, A. The discovered painting decoration of the Vorontsov Palace in St. Petersburg: Spectroscopic characterization in support of conservation. *J. Phys. Conf. Ser.* **2019**, *1410*, 012172. [CrossRef]
39. Fanost, A.; Gimat, A.; de Viguerie, L.; Martinetto, P.; Giot, A.-C.; Clémancey, M.; Blondin, G.; Gaslain, F.; Glanville, H.; Walter, P.; et al. Revisiting the identification of commercial and historical green earth pigments. *Colloids Surf. A Physicochem. Eng. Asp.* **2020**, *584*, 124035. [CrossRef]
40. Fratini, F.; Cantisani, E.; Pecchioni, E.; Pandeli, E.; Vettori, S. *Pietra Alberese*: Building Material and Stone for Lime in the Florentine Territory (Tuscany, Italy). *Heritage* **2020**, *3*, 1520–1538. [CrossRef]

41. Haynes, H.; O'Neill, R.; Neff, M.; Mehta, P.K. Salt Weathering Distress on Concrete Exposed to Sodium Sulfate Environment. *ACI Mater. J.* **2008**, *105*, 35–43.
42. Lubelli, B.; Van Hees, R.P.J.; Groot, C.W.P. Investigation on the behaviour of a restoration plaster applied on heavy salt loaded masonry. *Constr. Build. Mater.* **2006**, *20*, 691–699. [CrossRef]
43. Camuffo, D.; Bertolin, C.; Amore, C.; Bergonzini, A.; Brimblecombe, P. Thenardite-Mirabilite cycles in historical buildings. In Proceedings of the 9th Indoor Air Quality Meeting, Chalon-sur-Saone, France, 21–23 April 2010.
44. Marszałek, M.; Dudek, K.; Gaweł, A. Cement Render and Mortar and Their Damages Due to Salt Crystallization in the Holy Trinity Church, Dominicans Monastery in Cracow, Poland. *Minerals* **2020**, *10*, 641. [CrossRef]
45. Ordóñez, S.; La Iglesia, Á.; Louis, M.; García-Del-Cura, M.Á. Mineralogical evolution of salt over nine years, after removal of efflorescence and saline crusts from Elche's Old Bridge (Spain). *Constr. Build. Mater.* **2016**, *112*, 343–354. [CrossRef]
46. Eastaugh, N.; Walsh, V.; Chaplin, T.; Siddal, R. *Pigment Compendium: A Dictionary and Optical Microscopy of Historical Pigments*; Taylor and Francis: Oxford, UK, 2008; 968p.
47. Sonoda, N.; Rioux, J.P.; Duval, A.R. Identification des materiaux synthetiques dans les peintures modernes. II. Pigments organiques et matière picturale. *Stud. Conserv.* **2013**, *38*, 99–127. [CrossRef]
48. Magrini, D.; Bartolozzi, G.; Bracci, S.; Carlesi, S.; Cucci, C.; Picollo, M. Evaluation of the efficacy and durability of the "barium hydroxide method" after 40 years. Multi-analytical survey on the Crocifissione by Beato Angelico. *J. Cult. Herit.* **2020**, *45*, 362–369. [CrossRef]
49. Gliozzo, E.; Ionescu, C. Pigments—Lead-based whites, reds, yellows and oranges and their alteration phases. *Archaeol. Anthropol. Sci.* **2022**, *14*, 17. [CrossRef]
50. Arcolao, C.; Dal Bo', A. L'influenza delle sostanze proteiche naturali su alcune proprietà degli stucchi. In Proceedings of the Conference Studies Scienza e Beni Culturali, Lo Stucco: Cultura, Tecnologia, Conoscenza, Bressanone, Italy, 10–13 July 2001; pp. 527–538.